A model-free method for learning flexibility capacity of loads providing grid support

Austin R. Coffman*,† and Prabir Barooah*

Abstract—Flexible loads are a resource for the Balancing Authority (BA) of the future to aid in the balance of power supply and demand. In order to be used as a resource, the BA must know the capacity of the flexible loads to vary their power demand over a baseline without violating consumers' quality of service (QoS). Existing work on capacity characterization is model-based: They need models relating power consumption to variables that dictate QoS, such as temperature in case of an air conditioning system. However, in many cases the model parameters are not known or difficult to obtain. In this work, we pose a data driven capacity characterization method that does not require model information, it only needs access to a simulator. The capacity is characterized as the set of feasible spectral densities (SDs) of the demand deviation. The proposed method is an extension of our recent work on SD-based capacity characterization that was limited to linear time invariant (LTI) dynamics of loads. The method proposed here is applicable to nonlinear dynamics. Numerical evaluation of the method is provided, including a comparison with the model-based solution for the LTI case.

I. INTRODUCTION

The future of the power grid is green: an increased reliance on renewable generation. This can pose a challenge for Balancing Authorities (BAs) since renewable generation is volatile. To ensure balance of power in the presence of this volatility, BAs need additional sources of energy storage. Apart from batteries, a new resource has been the subject of much investigation for its ability to provide battery-like service: flexible loads.

Most loads have some flexibility in power demand: they can deviate their power demand from a baseline value without violating their quality of service (QoS). The BA would request this demand deviation, termed the *reference signal*, so to help balance the grid. The baseline consumption is then power consumption in absence of any requests from the BA. Examples of flexible loads include pumps for pool cleaning [1] and agricultural purposes [2], TCLs [3], and HVAC equipment [4].

If the grid operator expects the flexible loads to track the reference signal accurately, then the reference must not cause the loads to violate their QoS. From the viewpoint of the grid operator, flexible loads not tracking a reference makes them appear unreliable. From the viewpoint of the load, reference signals that continually require QoS violation

ARC and PB are with the Dept. of Mechanical and Aerospace Engineering, University of Florida, Gainesville, FL 32601, USA. The research reported here has been partially supported by the NSF through awards #1646229 and #1934322.

provide incentive for loads to stop providing grid support. In either case, avoidance of the above scenarios is paramount to the long term success of grid support from flexible loads. That is, reference signals must be designed to respect the *capacity* of the collection of flexible loads.

Informally, the capacity of of a flexible load represents limitations in its ability to track a demand deviation reference signal due to QoS requirements at the individual loads. Consequently, a key step in determining the capacity is relating the QoS requirements to requirements for the reference signal for demand deviation. This is a challenging task; various approaches have been proposed in recent years [5]–[12]. A popular approach is to develop ensemble level necessary conditions [5], [7]. Reference signals that satisfy these conditions ensure the ability of all loads in the collection to satisfy QoS while tracking the reference. Other approaches include geometry based characterizations [13], characterizations through distributed optimization [14], and characterizations that approximate the Minkowski sum of individual load's "resource polytopes" [15]–[17].

In addition to the previous references, there is an emerging methodology of characterizing the capacity as constraints on the statistics of the reference signal [18]–[20], rather than the reference signal itself. Most commonly, as constraints on the *spectral density* (SD) of the reference signal [19], [20]. Elaborating, these methods aim to precisely quantify the regions shown in Figure 1 based on the QoS of the loads considered. One particular advantage of these characterizations is that they are suitable for long term resource allocation. That is, such a characterization can answer questions such as: how many flexible loads will a BA require if it invests in 10% more solar? Contrarily, if the capacity of the flexible loads is characterized in the time domain, the BA would then have to predict many months in advance solar and flexible load trajectories to see if the flexible loads can deliver.

Irrespective of statistical or time domain characterizations, many of the listed works have one thing in common: they are model based. Meaning, they need a model that relates demand deviation of the flexible load(s) to QoS. The computed capacity of the load(s) depend on the model/model parameters. In addition, most of the existing methods require the models to be linear time invariant (LTI). An LTI model may be inappropriate for certain loads. Even if a linear model is appropriate, the parameters of the flexible load model are typically unknown or require estimation from experimental data or high-fidelity simulations. In the spirit of model free control, one might wonder then, is it possible to directly estimate a characterization of flexible load capacity from

^{*} University of Florida

[†] corresponding author, email: bubbaroney@ufl.edu.

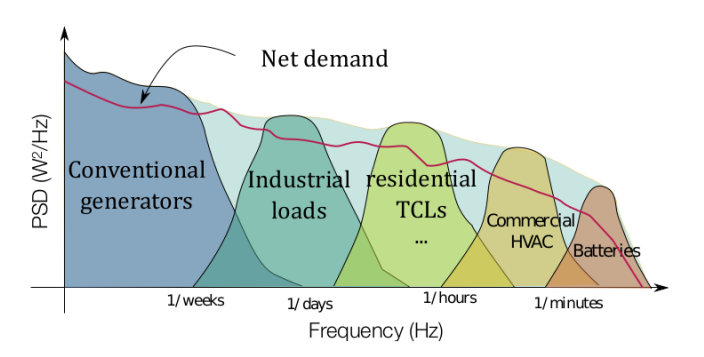


Fig. 1: An example spectral allocation of resources to meet the grids needs.

data?

In this work, we develop a data-driven (model free) framework to determine flexible load capacity directly from data. That is, instead of relying on model knowledge it rather relies on access to a simulator to determine the capacity. This framework builds off of our past work [20], where we characterize the capacity of flexible load(s) as constraints on the SD of their power deviation. In the past work, to obtain a SD we set up an optimization problem: the BA projects its needs (roughly, the SD of net demand, e.g., shown in Figure 1) onto the constraint set of feasible of SD's. In [20], the models relating demand deviation to QoS variables were assumed LTI, and it was shown how to solve the optimization problem for that case.

We depart from our previous work here and venture into new territory by showing how to solve the projection problem from our past work without having access to model information, as long as we have the ability to generate data from a simulator. The key insight that allows for this model free construction is the choice of approximation architecture when discretizing the infinite dimensional optimization problem. This data driven framework also has the ability to accommodate non-linear flexible load models, whereas our past work [20] was for linear models only.

We validate our data driven framework in simulation examples. First, we compare the proposed data driven framework to the model based framework of our past work [20]. We then use our framework to estimate the capacity of a flexible load with a non-linear model.

The paper proceeds as follows. In Section II we introduce the method from our prior work. In Section III we introduce our data-driven method. Numerical experiments are conducted in Section IV and we conclude in Section V

II. SPECTRAL CHARACTERIZATION OF QOS CONSTRAINTS

The symbol t is used to denote the continuous time while k is used to denote a discrete time index. The sampling interval is Δt .

A. Deterministic QoS constraints

Denote by P[k] the power consumption of a flexible load at time index k, and let $P^b[k]$ its baseline demand. The demand deviation is $\tilde{P}[k] := P[k] - P^b[k]$. The load provides grid support service by controlling the deviation $\tilde{P}[k]$ to track a desired deviation signal, called a reference, while maintaining its own QoS. The first QoS constraint is simply an actuator constraint:

QoS-1:
$$\left| \tilde{P}[k] \right| \le c_1, \quad \forall \ k,$$
 (1)

where the constant c_1 , the maximum possible deviation of power consumption, depends on the rated power and the baseline demand. Second, define the demand increment $\tilde{P}_{\delta}[k] := \tilde{P}[k] - \tilde{P}[k-\delta]$, where $\delta > 0$ is a predetermined (small) integer time interval. The second constraint is a ramping rate constraint:

QoS-2:
$$\left| \tilde{P}_{\delta}[k] \right| \le c_2, \quad \forall \ k.$$
 (2)

Third, define the additional energy use during any integer time interval of length T:

$$\tilde{E}[k] = \sum_{\sigma=k-T+1}^{k} \tilde{P}[\sigma]. \tag{3}$$

The third QoS constraint is that

QoS-3:
$$\left| \tilde{E}[k] \right| \le c_3, \quad \forall \ k.$$
 (4)

The parameter T in (3) can represent the length of a billing period. Ensuring (4) ensures that the energy consumed during a billing period close to the nominal energy consumed, although it is stronger than what is necessary.

To define the fourth and last QoS constraint, we associate with the VES system a *storage variable* $\tilde{x}[k]$ that is related to the demand deviation, and impose the constraint

QoS-4:
$$|\tilde{x}[k]| \le c_4, \quad \forall \ k.$$
 (5)

1) Understanding QoS-4: To understand the storage variable, imagine a flexible HVAC system providing VES. We first present a model of the HVAC systems internal temperature T_z in continuous time, as it is more naturally presented in this setting. This model is:

$$C\frac{dT_z(t)}{dt} = \frac{1}{R}(T_a(t) - T_z(t)) + \dot{q}_{int}(t) + Q(t),$$
 (6)

where C and R are thermal capacitance and resistance, $T_a(t)$ is the ambient temperature, and $\dot{q}_{\rm int}(t)$ is an exogenous disturbance. The quantity Q(t) is the rate of heat delivered to the building by the HVAC system (negative if cooling).

We consider two models, one linear and the other nonlinear for relating the electrical power deviation to the indoor temperature. In both cases a temperature deviation will play the role of the storage variable $\tilde{x}[k]$.

a) Linear model: Suppose $Q(t)=-\eta_0 P(t)$ where η_0 is the coefficient of performance (COP) under design conditions. In general, the baseline power consumption for a HVAC system is the value $P^b(t)$ that keeps the internal temperature of the load at a fixed value \bar{T} , which for (6) is

$$P^{b}(t) = -\frac{\left(T_{a}(t) - \bar{T}\right)}{\eta_{0}R} - \frac{\dot{q}_{\text{int}}(t)}{\eta_{0}}.$$
 (7)

Since we are concerned with the flexibility in the load, we linearize (6) about the thermal setpoint $\bar{\theta}$ and the baseline power $P^b(t)$ yielding,

$$\dot{\tilde{T}}_z(t) = -\gamma \tilde{T}_z(t) + \beta \tilde{P}(t), \quad \gamma = \frac{1}{RC}, \quad \beta = \frac{\eta_0}{C},$$
 (8)

where $\tilde{T}_z \triangleq T_z(t) - \bar{T}$ is the internal temperature deviation and \tilde{P} is as defined at the beginning of this Section. The corresponding discrete-time dynamic model relating $\tilde{P}[k]$ to $\tilde{T}_z[k]$ is

$$\tilde{T}_z[k+1] = a\tilde{T}_z[k] + b\tilde{P}[k],\tag{9}$$

(where $a=e^{-\gamma\Delta t}$ and $b=\beta\int_0^{\Delta t}e^{-\gamma\tau}d\tau$), which is also a first order linear time invariant (LTI) model.

b) Nonlinear model: A more realistic model is a COP that varies depending on the difference between indoor and outdoor temperature. When the HVAC system is providing cooling, the hotter the outside is compared to the indoors, the less efficient the HVAC system is in rejecting heat from the cooler indoor to the hotter outdoor [21]. Such a situation can be modeled as

$$\eta(t) = \eta_0 - \alpha_1 \left(T_a - T_z(t) \right) + \alpha_2. \tag{10}$$

The role of the constant α_2 is to get $\eta(t)=\eta_0$ when T_a and T_z are both constant and equal to the values the HVAC system is designed for. The dynamic equation (6) with this model for the COP then becomes the following nonlinear ODE

$$C\dot{T}_z = -\frac{1}{R} \left(T_a - T_z(t) \right) + \dot{q}_{int}(t)$$

$$+ \left(\eta_0 - \alpha_1 \left(T_a - T_z(t) \right) + \alpha_2 \right) P(t).$$
 (11)

The baseline for this model is the expression (7), except replacing η_0 with $\bar{\eta} = \eta_0 - \alpha_1 \left(T_a - \bar{T} \right) + \alpha_2$. The corresponding ODE that relates the power deviation $\tilde{P}(t)$ to temperature deviation $\tilde{T}_z(t)$ is the following bilinear ODE:

$$C\frac{d\tilde{T}_z(t)}{dt} = -\frac{1}{R}\tilde{T}_z(t) + \left(\eta_0 - \alpha_1(T_a - \bar{T}_z(t)) + \alpha_2\right)\tilde{P}(t) + \alpha\tilde{P}\tilde{T}_z(t) + \alpha\tilde{T}_z(t)\tilde{P}(t). \tag{12}$$

The derivation is tedious but straightforward, so it is omitted due to space limitations. The corresponding discrete time model - obtained with 1st order Euler backward discretization - is also a bilinear dynamic system.

B. Mathematical Preliminaries

In our prior work [22], we had developed a methodology that characterizes the capacity of a flexible load in the frequency domain. We briefly discuss this prior work here. Denote the power consumption of a flexible load as $\tilde{P}[k]$, where we model \tilde{P} as a stochastic process. The mean and autocorrelation function for \tilde{P} are,

$$\mu_{\tilde{P}}[k] \triangleq \mathsf{E}[\tilde{P}[k]], \qquad \forall k,$$
 (13)

$$R_{\tilde{P}}[s,k] \triangleq \mathsf{E}[\tilde{P}[s]\tilde{P}[k]], \quad \forall \ s, \ k,$$
 (14)

where $E[\cdot]$ denotes mathematical expectation. In the past work, we made the following assumption about the stochastic process \tilde{P} .

Assumption 1. The stochastic process \tilde{P} is wide sense stationary (WSS) with mean function $\mu_{\tilde{P}}[k] = 0$ for all k.

Under this assumption we have that the autocorrelation function will solely be a function of $\tau = s - k$. In this case, the autocorrelation function is an asymmetric Fourier transform pair with the Spectral Density:

$$R_{\tilde{P}}(\tau) = \frac{1}{2\pi} \int_{-\pi}^{\pi} S_{\tilde{P}}(\Omega) e^{j\Omega\tau} d\Omega$$
, and (15)

$$S_{\tilde{P}}(\Omega) = \sum_{\tau = -\infty}^{\infty} R_{\tilde{P}}[\tau] e^{-j\Omega\tau}, \tag{16}$$

where $S_{\tilde{P}}(\Omega)$ is the (power) Spectral Density (SD) of \tilde{P} , $\omega \in [-\pi,\pi]$ is the frequency variable, and j is the imaginary unit. The above is based on the general definition of the SD of the signal \tilde{P} ,

$$S_{\tilde{P}}(\Omega) \triangleq \lim_{N \to \infty} \frac{1}{N} \mathsf{E} \left[\left| \sum_{k=1}^{N} \tilde{P}[k] e^{-j\Omega k} \right|^{2} \right] \tag{17}$$

the equivalence of definitions (17) and (16) for a WSS process is the Wiener-Khinchin theorem. Since the mean function of \tilde{P} is zero for all time we have

$$\sigma_{\tilde{P}}^2 = R_{\tilde{P}}(0) = \frac{1}{2\pi} \int_{-\pi}^{\pi} S_{\tilde{P}}(\Omega) d\Omega, \tag{18}$$

that is, the variance $\sigma_{\tilde{P}}^2$ of \tilde{P} is the integral of the (power) SD. To illustrate our method from prior work we will also make use of the Chebyshev inequality for a r.v. X:

$$\mathsf{P}(|X - \mu_X| \ge C) \le \frac{\sigma_X^2}{C^2}, \quad \forall \ C > 0, \tag{19}$$

where $P(\cdot)$ denotes probability. Another useful relation is the following:

Proposition 1. If the input x[k] to a linear time invariant system with frequency response $H(e^{j\Omega})$ is WSS and has SD Φ_x , then the output y[k] is also WSS and its SD Φ_y is given by $\Phi_y(\Omega) = \Phi_x(\Omega)|H(e^{j\Omega})|^2$.

C. Probabilistic QoS Constraints and SD-based Capacity Characterization

Each QoS constraint potentially involves a distinct signal. In QoS-1, the signal is the power deviation $\tilde{P}[k]$ itself. In QoS-3, it is the storage variable $\tilde{x}[k]$. We denote by $Z_{\ell}[k]$ the signal relevant for the ℓ -th QoS constraint. In each QoS, the relevant signal is related to the power deviation $\tilde{P}[k]$, and we denote by \mathcal{G}_{ℓ} the (potentially dynamic) system that relates the input \tilde{P} to the output Z_{ℓ} .

Next we illustrate how to pose the QoS constraints as constraints on SDs. We start by considering the ℓ -th QoS, which we re-formulate as

$$P(|Z_{\ell}[k]| \ge c_{\ell}) \le \varepsilon_{\ell}, \quad \forall k \tag{20}$$

where $\varepsilon_{\ell} \ll 1$ is the tolerance. From the Chebyshev inequality (19) and the equation (18) we have:

$$\frac{1}{2\pi} \int_{-\pi}^{\pi} S_{Z_{\ell}}(\Omega) d\Omega \le c_{\ell}^{2} \varepsilon_{\ell} \implies \mathsf{P}\left(|Z_{\ell}[k]| \ge c_{\ell}\right) \le \varepsilon_{\ell}. \tag{21}$$

Thus, the probabilistic constraint (20) can be assured by asking for the following constraint involving SD of Z_{ℓ} to be satisfied:

$$\frac{1}{2\pi} \int_{-\pi}^{\pi} S_{Z_{\ell}}(\Omega) d\Omega \le b_{\ell} =: c_{\ell}^{2} \varepsilon_{\ell}. \tag{22}$$

If the dynamic system \mathcal{G}_{ℓ} relating the input \tilde{P} and output Z_{ℓ} were a linear time invariant system, then (23) can be translated to a constraint on the power deviation:

$$\frac{1}{2\pi} \int_{-\pi}^{\pi} S_{\tilde{P}}(\Omega) |G_{\ell}(e^{j\Omega})|^2 d\Omega \le b_{\ell} \tag{23}$$

where $G_{\ell}(e^{j\Omega})$ is the frequency response of the dynamic system \mathcal{G}_{ℓ} . In the general case with m constraints, the constraint set for the SD $S_{\tilde{P}}$ is

$$\mathcal{S} \triangleq \left\{ S_{\tilde{P}} \mid \frac{1}{2\pi} \int_{-\pi}^{\pi} S_{Z_{\ell}}(\Omega; S_{\tilde{P}}) d\Omega \leq b_{\ell}, \quad \ell = 1, \dots, m \right\}.$$
(24)

The notation $S_{Z_\ell}(\Omega;S_{\tilde{P}})$ above is used to emphasize that the SD of the signal Z_ℓ is a function of $S_{\tilde{P}}$, the SD of $\tilde{P}[k]$. The function can be arbitrarily complex when the dynamic models \mathcal{G}_ℓ are nonlinear.

As long as the SD of the demand deviation $\tilde{P}[k]$ belong to the set \mathcal{S} , each of the ℓ probabilistic QoS constraints - such as QoS 1-4 described in Section II-A - holds. Thus, the set \mathcal{S} also represents the demand deviation capacity of the flexible load.

Now, denote by \mathcal{H} the set of SDs defined over $[-\pi, \pi)$, and define the function $B_{\ell} : \mathcal{H} \to \mathbb{R}^+$ as

$$\bar{B}_{\ell}(S_{\tilde{P}}) = \frac{1}{2\pi} \int_{-\pi}^{\pi} S_{Z_{\ell}}(\Omega; S_{\tilde{P}}) d\Omega \tag{25}$$

and the array $\bar{B}(S_{\tilde{P}}) = [\bar{B}_1(S_{\tilde{P}}), \ldots, \bar{B}_m(S_{\tilde{P}})]^T \in \mathbb{R}^m$. By denoting $\mathsf{b} = [\varepsilon_1 c_1^2, \ldots, \varepsilon_m c_m^2]^T \in \mathbb{R}^m$ the constraint $S_{\tilde{P}} \in \mathcal{S}$ can be represented as

$$\bar{B}(S_{\tilde{P}}) \le \mathsf{b}.$$
 (26)

Now consider the following optimization problem:

$$\min_{S} \quad \frac{1}{2\pi} \int_{-\pi}^{\pi} \left(S(\Omega) - S^{\text{BA}}(\Omega) \right)^{2} d\Omega$$
s.t. $\bar{B}(S_{\bar{D}}) \leq \mathsf{b}$ and $S(\Omega) \geq 0 \quad \forall \ \Omega \in [-\pi, \pi),$ (27)

where $S^{\text{BA}}(\Omega)$ is the spectral density of the stochastic process that generates the reference signals from the BA. How to determine $S^{\text{BA}}(\Omega)$ is discussed in the next section. We define the capacity of the flexible load as the solution $S_{\tilde{P}}^*$ of the optimization problem (27).

1) BA's spectral needs: The total needs of the BA is encapsulated by the SD of the net demand signal, an example of which is shown in Figure 1. With historical data, a BA can estimate the SD of the net demand signal, which we denote as $S^{\rm ND}(\Omega)$. Any well posed estimation technique can be applied. All controllable resources, including generators, flywheels, batteries, and flexible loads, together have to supply $S^{\rm ND}(\Omega)$. To determine solely the portion of $S^{\rm ND}(\Omega)$ that flexible loads should contribute to we "filter" $S^{\rm ND}(\Omega)$. That is, with $F(e^{j\Omega})$ an appropriate filter we have

$$S^{\text{BA}}(\Omega) = \left| F(e^{j\Omega}) \right|^2 S^{\text{ND}}(\Omega). \tag{28}$$

The quantity S^{BA} is the frequency domain analog of the reference signal r[k] that will be asked from the loads, and will be referred to as the *reference SD* in the sequel.

D. Linear time invariant (model-based) case: prior work

Now we consider the scenario when the \mathcal{G}_ℓ 's are LTI systems. Recall that $S_{Z_\ell}(\Omega; \tilde{P})$ in the definition of $B(\cdot)$ in (25) is the SD of $Z_\ell[k]$, which in turn is the output of the system \mathcal{G}_ℓ when driven by an input signal whose SD is $S_{\tilde{P}}(\Omega)$. Since the system \mathcal{G}_ℓ is LTI with frequency response $G_\ell(e^{j\Omega})$, it follows from Prop. 1 that

$$S_{Z_{\ell}}(\Omega) = |G_{\ell}(e^{j\Omega})|^2 S_{\tilde{P}}(\Omega), \tag{29}$$

and plugging it in (25) we get

$$\bar{B}_{\ell}(S_{\tilde{P}}) = \frac{1}{2\pi} \int_{-\pi}^{\pi} |G_{\ell}(e^{j\Omega})|^2 S_{\tilde{P}}(\Omega) d\Omega. \tag{30}$$

The constraints in Problem (32) are thus linear in the decision variable $S_{\tilde{P}}(\Omega)$. Since the objective is quadratic in the decision variable, the problem is a quadratic problem, although infinite dimensional.

Remark 1. The problem (32) can be reduced to a tractable finite dimensional optimization problem by discretizing the continuous frequency Ω into N points on the unit circle. The decision vector of the optimization problem becomes N. The resulting problem is a finite dimensional quadratic program (QP) that can be efficiently solved using readily available NLP solders. In all such problems in the rest of the paper that involve functions of continuous frequency Ω over $[-\pi, \pi]$, we assume that such a discretization is done to convert the problem to a finite dimensional problem.

The finite dimensional QP alluded to in Remark 1 is the problem posed and solved in our prior work [20]. Thus,

the optimization problem needed to characterize capacity is fairly straightforward to solve, as long as the models \mathcal{G}_{ℓ} 's are LTI and the model parameters are known. There are two weaknesses. The first is that a linear model may not be appropriate for certain types of flexible loads. The second is that even if a LTI model is sufficiently accurate, obtaining the model parameters is not an easy task. Take the LTI model (9) of temperature deviation in a building. This equation alone is actually quite merited for this particular application, and there is a plethora of work spanning back to the 1980's [23] on using ODEs of this form to model the dynamics in certain flexible loads. These works almost solely focus on estimating the parameters of the model such as (9). These parameters are challenging to estimate. Despite this, many current capacity characterizations explicitly depend on the parameters such as R and C.

III. PROPOSED DATA DRIVEN METHOD

The goal of this section will be to develop an algorithm that can solve the problem (27) using data that can come from experiments or simulations, but without requiring (i) that the underlying systems \mathcal{G}_{ℓ} 's are LTI and (ii) any knowledge of the models \mathcal{G}_{ℓ} 's. Only a simulator that can simulate \mathcal{G}_{ℓ} 's for various inputs is needed.

To facilitate our algorithm, we first elect a function approximation architecture for the decision variable S in the optimization problem (27). With our form of function approximation, we show how to obtain an estimate of all of the ingredients needed to solve (27) with solely data.

A. Function approximation

We consider linear function approximations, that is, we approximate the decision variable S in (27) through

$$S^{\theta}(\Omega) = \sum_{i=1}^{d} \psi_i(\Omega)\theta_i = \Psi^T(\Omega)\theta, \tag{31}$$

where each basis $\psi_i(\Omega)$ is a SD, and $\theta \geq 0$. The number of basis functions, d, is a design choice. We use $\Psi^T\theta$ to denote the entire trajectory $\{\Psi^T(\Omega)\theta\}_{\Omega=-\pi}^{\Omega=\pi}$.

We then transform the optimization problem (27) over S to one over the finite dimensional vector $\theta \in \mathbb{R}^d$. The problem (27) is transformed to a finite dimensional non-linear program (NLP):

$$\begin{split} \theta^* &= \arg\min_{\theta} & \ \frac{1}{2\pi} \int_{-\pi}^{\pi} \left(\Psi^T(\Omega) \theta - S^{\text{BA}}(\Omega) \right)^2 d\Omega \\ & \text{s.t.} & \ B(\theta) \leq \text{b}, \quad \text{and} \quad \theta \geq 0, \end{split}$$
 (32)

where $B(\theta) := \bar{B}(\Psi^T \theta)$, where $\bar{B}(\cdot)$ is defined in (25). Since $\psi_i(\Omega) \geq 0$ for each i, requiring $\theta \geq 0$ ensures that $\Psi^T(\Omega)\theta$ satisfies the properties of SDs (non-negativity and even) and so the search is limited to SDs, and the solution obtained by solving the problem (32), $\Psi^T(\Omega)\theta^*$, is guaranteed to be a SD.

B. Estimating $B(\theta)$ from data

The method we propose for estimating $B_{\ell}(\theta)$ for a given θ and a fixed ℓ is given below. It is then repeated for $\ell = 1, \ldots, m$ to obtain $B(\theta)$

- 1) Generate samples of the ℓ -th QoS signal, $Z_{\ell}[k]$, when power deviation $\tilde{P}[k]$ has SD $\Psi^{T}(\Omega)\theta$. This is done in two steps:
 - a) Input generation: For each i ($i=1,\ldots,d$) generate a colored noise sequence $\varphi_i[k]$ with SD $\theta_i\Psi_i(\Omega)$. (This can be done in many ways. One possibility is to perform a spectral factorization of Ψ_i to obtain a filter $H(e^{j\Omega})$ so that $|H(e^{j\Omega})|^2 = \Psi_i(\Omega)$. Passing a zero mean unit variance white noise through will generate a WSS process with SD $\Psi_i(\Omega)$ due to Prop. 1. Multiplying this sequence with $\sqrt{\theta_i}$ will produce the desired sequence $\varphi[k]$. Another method is to take the inverse (discrete time) Fourier transform of the SD multiplied pointwise (in the frequency domain) by random phase.)
 - b) Output generation: Use a simulator of the system $\overline{\mathcal{G}_{\ell}}$ to generate $\overline{Z_{i,\ell}}[k]$ by using the input $\varphi_i[k]$, for each i, and then sum over i to obtain $Z_{\ell}[k] := \sum_{i=1}^{d} Z_{i,\ell}[k]$. (Because the same simulator is used for each i, we have $Z_{\ell}[k] = \mathcal{G}_{\ell}(u)[k]$ where $u[k] = \sum_{i} \varphi_i[k]$. Because the processes $\varphi_i[k]$ and $\varphi_j[k]$ are uncorrelated for $i \neq j$, the SD of u is the sum of the SDs of $\varphi_i[k]$'s, which is equal to $\Psi^T(\Omega)\theta$ by design. Thus, the SD of $Z_{\ell}[k]$ is SD of the output of \mathcal{G}_{ℓ} with an input whose SD is $\Psi^T(\Omega)\theta$. In other words, the SD of $Z_{\ell}[k]$ is $S_{Z_{\ell}}(\Omega; \Psi^T(\Omega)\theta)$.)
- 2) Estimate the function value $B_\ell(\theta)$ from the samples $Z_\ell[k]$ by utilizing the Wiener-Khinchin theorem. Namely,

$$\hat{S}_{Z_{\ell}}(\Omega; \Psi^T \theta) = \hat{\mathsf{E}} \left[\frac{1}{N} \Big| \sum_{k=1}^{N} Z_{\ell}[k] e^{-j\Omega k} \Big|^2 \right], \quad (33)$$

$$\hat{B}_{\ell}(\theta) = \frac{1}{2\pi} \int_{-\pi}^{\pi} \hat{S}_{Z_{\ell}}(\Omega; \Psi^T \theta) d\Omega \tag{34}$$

where $\hat{E}[\cdot]$ is a shorthand for an estimate of the expectation $E[\cdot]$. In particular, the estimate is obtained by performing multiple simulations, computing the quantity inside the square braces in the right hand side of (33) in each simulatin, and averaging over those simulations.

A graphical illustration of the data generation step of the algorithm is shown in Figure 2. To completely specify the problem (32), the quantity $S^{\rm BA}(\Omega)$ is required. As mentioned in section II-C1, it can be estimated using net load data.

The problem (32) is a finite dimensional NLP, with a d-dimensional decision vector θ . However, standard NLP solvers cannot be easily used in the general nonlinear case. Since the SD of the output $Z_{\ell}[k]$ can be an arbitrarily

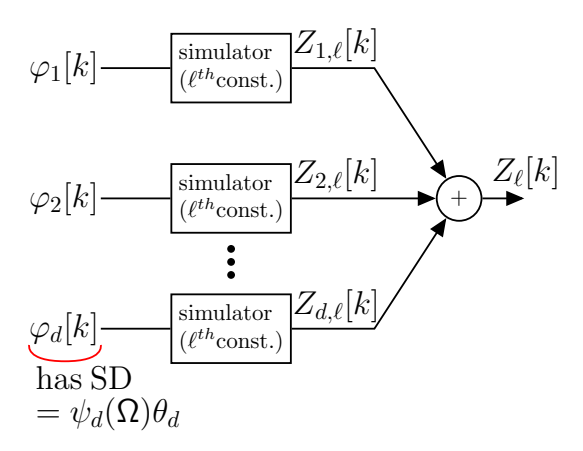


Fig. 2: Generating the ℓ -th QoS signal $Z_{\ell}[k]$.

complicated function of θ , the gradient and/or Hessian of the function $B(\theta)$ is not readily available. They can be numerically estimated, or a gradient free method can be used. In the special case when the systems \mathcal{G}_{ℓ} 's are LTI, the problem becomes a QP, a convex problem that can be easily solved. We describe this special case in Section III-C.

Remark 2. Key in our ability to remove dependence on the model knowledge is the requirement that each basis function Ψ_i is in fact a SD. Without this form of function approximation it may be difficult to develop a truly model free form of the problem (27). As we will discuss next, this model free dependence rids us of the limitations of the past work discussed in Section II-D.

C. The LTI case

Since $S_{\tilde{P}} = \Psi^T \theta$, it follows from (25) that

$$\bar{B}_{\ell}(\theta) = B_{\ell}(\Psi^T \theta) = \frac{1}{2\pi} \int_{-\pi}^{\pi} S_{Z_{\ell}}(\Omega; \Psi^T \theta) d\Omega.$$
 (35)

Recall that $S_{Z_{\ell}}(\Omega; \Psi^T \theta)$ is the SD of $Z_{\ell}[k]$ which is the output of system \mathcal{G}_{ℓ} when driven by a signal whose SD is $\Psi^T(\Omega)\theta$. Since the system \mathcal{G}_{ℓ} is LTI with frequency response $G_{\ell}(e^{j\Omega})$, it follows from Prop 1 that

$$S_{Z_{\ell}}(\Omega) = |G_{\ell}(e^{j\Omega})|^2 \Psi^T(\Omega)\theta. \tag{36}$$

Plugging it back in (35) we get

$$\bar{B}_{\ell}(\theta) = \left[\frac{1}{2\pi} \int_{-\pi}^{\pi} |G_{\ell}(e^{j\Omega})|^2 \Psi^T(\Omega) d\Omega \right] \theta \qquad (37)$$

Stacking these $\bar{B}_{\ell}(\theta)$'s, we obtain

$$\bar{B}(\theta) = B\theta \tag{38}$$

where $B \in \mathbb{R}^{m \times d}$ is

$$B = \frac{1}{2\pi} \int_{-\pi}^{\pi} \mathsf{G}(\Omega) \Psi^{T}(\Omega) d\Omega, \tag{39}$$
$$\mathsf{G}(\Omega) = [|G_{1}(e^{j\Omega})|^{2}, \dots, |G_{m}(e^{j\Omega})|^{2}]^{T}$$

TABLE I: Simulation parameters

	Par.	Unit	Value	Par.	Unit	Value
١	R	°C/kW	8	C	kWh/°C	22
İ	T	hours	5	$\{\epsilon_i\}_{i=1}^4$	N/A	0.05
İ	c_1	kW	40	c_2	kW	8
İ	c_3	°C	1	c_4	kWh	8
İ	η_0	N/A	3.5	T_a	°C	30
İ	δ	sec.	20	$\dot{q}_{ m int}$	kW	0

The objective function (32) can be expressed as

$$f(\theta) = \theta^T A \theta + C \theta + d, \tag{40}$$

where

$$A = \frac{1}{2\pi} \int_{-\pi}^{\pi} A(\Omega) d\Omega, \text{ with } A(\Omega) = \Psi(\Omega) \Psi^{T}(\Omega), \quad (41)$$

$$C = \frac{1}{2\pi} \int_{-\pi}^{\pi} C(\Omega) d\Omega$$
, with $C(\Omega) = \Psi(\Omega) S^{\text{BA}}(\Omega)$, (42)

$$d = \frac{1}{2\pi} \int_{-\pi}^{\pi} d(\Omega) d\Omega, \text{ with } d(\Omega) = \left(S^{\text{BA}}(\Omega)\right)^{2}. \tag{43}$$

To estimate the quantities C and d above, the quantity $S^{\text{BA}}(\Omega)$ is required. As mentioned in section II-C1, it can be estimated using net load data.

$$f(\theta) = \theta^T A \theta + C \theta + d. \tag{44}$$

The optimization problem (32) now becomes the following d-dimensional quadratic program (QP)

$$\theta^* = \arg\min_{\theta > 0} f(\theta), \quad \text{s.t.} \quad B\theta \le \mathsf{b}.$$
 (45)

To reiterate, in order to compute $f(\theta)$ and B, no model knowledge is required, only access to a simulator.

IV. NUMERICAL EXPERIMENTS

A numerical example of using the proposed data driven method to determine the capacity is illustrated in this section. The flexible loads considered are a collection of commercial building HVAC systems. We consider a homogeneous collection in this preliminary work. Each HVAC system in the collection has QoS 1-4 listed in Section II-A. The parameters are displayed in Table I, and are chosen so that the HVAC systems are representative of those in large commercial buildings (hence the large superscripts in Table I).

We first validate the proposed method by implementing it in the scenario in which the solution is known: when the models involved are LTI and are known. The solution is computed using the method from our prior work [20]. Next, we apply the method to data from a simulation that uses a non-linear model.

All relevant simulation parameters, if not specified otherwise, can be found in Table I. Note that the method does *not* have access to the R, C, and η_0 parameter values.

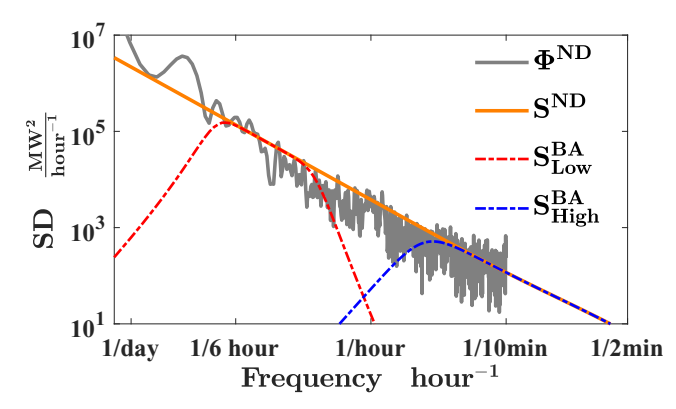


Fig. 3: Empirical net demand SD, modeled SD for BPA's net demand, and the two reference SD's for the high and low frequency passband.

A. BA's spectral needs

The net demand data is collected from BPA (a BA in the pacific northwest United States). The empirical SD of the net demand is determined using the method described in Section II-C1. We then fit an ARMA(2,1) model to the empirically estimated SD. Since the estimate $\Phi^{\rm ND}$ will cap out at the Nyquist frequency $1/10{\rm min}$, we extrapolate the net demand SD to the higher frequencies. The empirical SD (denoted $\Phi^{\rm ND}$) and the extrapolated net demand SD (denoted $S^{\rm ND}$) are shown in Figure 3.

We then choose two passbands to filter $S^{\rm ND}$: (i) a low passband [1/6,1/2] (1/hour) and (ii) a high passband [1/30,1] (1/min). The results of "filtering" (see eq. (28)) $S^{\rm ND}$ are also shown in Figure 3. The low passband SD is termed $S^{\rm BA}_{\rm Low}$ and roughly corresponds to the region for TCLs in Figure 1. The high passband SD is termed $S^{\rm BA}_{\rm High}$ and roughly corresponds to the region for HVAC systems in Figure 1.

B. Method Evaluation - LTI case

In this section we compare the data-driven method for the LTI case (Section III-C) with to solving the quadratic program (45) with full model knowledge, both to obtain θ^* . In both cases we use CVX [24] to solve the QP. We use the following basis SD's

$$\psi_i(\Omega) = \begin{cases} 1, & \text{if } \Omega \in [\hat{\Omega}_{i-1}, \hat{\Omega}_i). \\ 0, & \text{otherwise.} \end{cases}$$
 (46)

for $1 \leq i \leq d$. The set of points $\{\hat{\Omega}_i\}_{i=1}^d$ is a subset of the linearly spaced discrete frequency points on the unit circle. We consider n=2000 large commercial buildings as one large flexible load. The idea is to illustrate how much of the grids needs can be met by the collection. To do this, the two reference SDs obtained from the previous section are projected onto the *same* ensemble constraint set.

The results of this are shown in Figure 4, where the black dashed lines represent the model based solution. The two SD's are nearly identical.

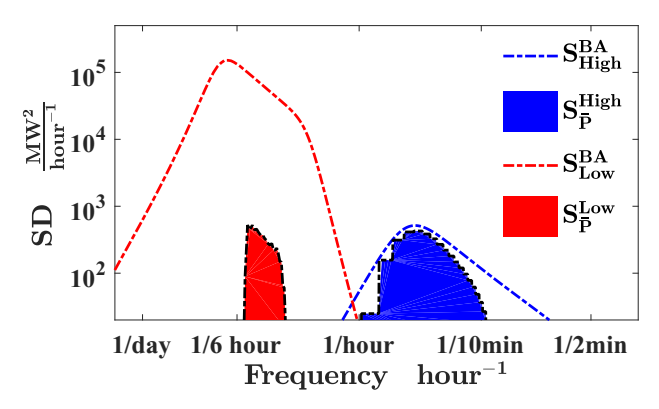


Fig. 4: LTI case: The two reference SDs and the corresponding capacity SDs (boundary of the shaded regions) obtained from the proposed method for a homogeneous collection of n=2000 loads. Black dashed lines represent model based solution.

C. Method Evaluation: Non-linear case

In this section we use the (discrete-time version of the) nonlinear dynamic model (12) relating power deviation to indoor temperature. In this scenario, all of the parameter values (except for now we have $\eta[k]$) remain the same as in the previous scenario and are given in Table I. The same basis SD's as in the previous scenario are also used here. We elect the value α appearing in (10) as $\alpha_1=0.15$ and $\alpha_2=1.175$.

The proposed method is applied to simulation data from the non-linear system. The reference SD is $S_{\rm Low}^{\rm BA}$ and n=15000. It is possible to use a standard NLP solver to solve (32), however we obtained positive results by applying the data driven algorithm in Section III-C to data collected from the nonlinear system. We feel this result is more interesting, and choose to show it here instead of results from the NLP solver. We emphasize that the method does not know anything about the model, it only uses simulation data. The results - the solution SD - is shown in Figure 5.

To verify that the solution provided by the method is meaningful, we generate power deviation trajectories with SD equal to the solution SD. Then the corresponding demand trajectories are used to simulate the model again using the simulator to compute the resulting temperature deviations. One such temperature trajectory is shown in Figure 5. We see from the figure that temperature is maintained within bounds during the time interval shown, indicating that the power deviation signal is within the capacity of the load.

V. CONCLUSION

We presented a data driven method to estimate the capacity of flexible load(s) as the optimal spectral density of demand deviation. Optimal here refers to being close to what the power grid needs. The method builds on our prior work [20] which was model-based and was limited to LTI models.

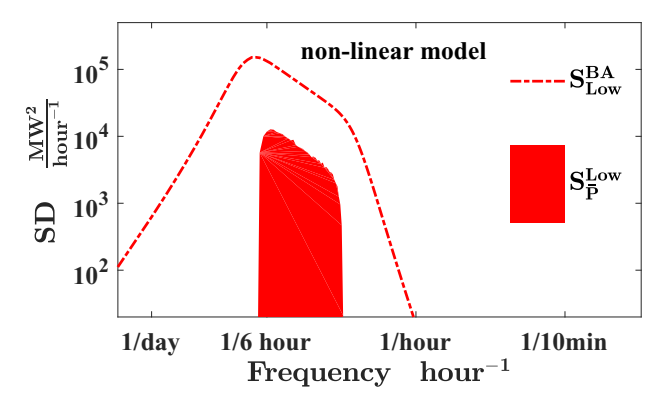


Fig. 5: Non linear case: The capacity (and reference) SD for n=15000 flexible loads, each with a non-linear model.

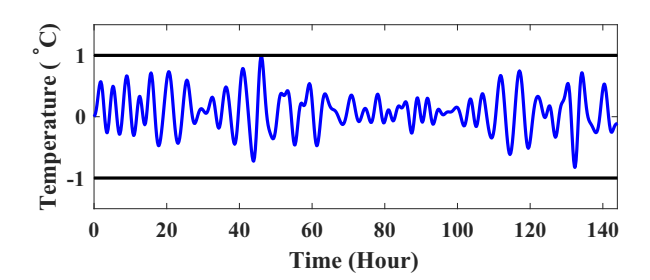


Fig. 6: Sample path of a flexible HVAC load's temperature deviation from setpoint (evolves according to (12)). The black lines represent the QoS constraint.

The method proposed here is also applicable to nonlinear dynamics, and more importantly, it does not need model knowledge. It only needs access to a simulator (or measurements of relevant data). The core of the algorithm is a function approximation architecture with basis functions that are chosen to be spectral densities. In simulations, our proposed data-driven method is validated against the model knowledge scenario; the results are positive.

Solving the projection problem in the nonlinear dynamics case is not trivial since symbolic derivatives with respect to the decision variables is not possible. This aspect of the method has room for improvement. Other avenues for future work include leveraging the data driven framework to: (i) estimate the capacity of heterogeneous ensembles of flexible loads and (ii) estimate the capacity under time varying weather conditions/disturbances.

REFERENCES

- [1] Y. Chen, M. U. Hashmi, J. Mathias, A. Bušić, and S. Meyn, "Distributed control design for balancing the grid using flexible loads," in *IMA Volume on the Control of Energy Markets and Grids*, 2017, pp. 1–26.
- [2] D. Kiedanski, D. Kofman, A. Orda, J. Horta, and A. Otero, "Exploiting flexibility in irrigation while maintaining optimal crop productivity," in 2019 IEEE International Conference on Communications, Control, and Computing Technologies for Smart Grids (SmartGridComm), 2019, pp. 1–7.

- [3] A. Khurram, R. Malhamé, L. Duffaut Espinosa, and M. Almassalkhi, "Identification of hot water end-use process of electric water heaters from energy measurements," *Electric Power Systems Research*, vol. 189, p. 106625, 2020.
- [4] J. Cai and J. E. Braun, "Laboratory-based assessment of HVAC equipment for power grid frequency regulation: Methods, regulation performance, economics, indoor comfort and energy efficiency," *Energy and Buildings*, vol. 185, pp. 148 161, 2019.
- [5] H. Hao, B. M. Sanandaji, K. Poolla, and T. L. Vincent, "Aggregate flexibility of thermostatically controlled loads," *IEEE Transactions on Power Systems*, vol. 30, no. 1, pp. 189–198, Jan 2015.
- [6] H. Hao, D. Wu, J. Lian, and T. Yang, "Optimal coordination of building loads and energy storage for power grid and end user services," *IEEE Transactions on Smart Grid*, vol. PP, no. 99, pp. 1–1, 2017.
- [7] A. Coffman, N. Cammardella, P. Barooah, and S. Meyn, "Aggregate capacity of TCLs with cycling constraints," arXiv preprint arXiv:1909.11497, 2019.
- [8] R. Yin, E. C. Kara, Y. Li, N. DeForest, K. Wang, T. Yong, and M. Stadler, "Quantifying flexibility of commercial and residential loads for demand response using setpoint changes," *Applied Energy*, vol. 177, pp. 149 – 164, 2016.
- [9] H. Hao, J. Lian, K. Kalsi, and J. Stoustrup, "Distributed flexibility characterization and resource allocation for multi-zone commercial buildings in the smart grid," in 2015 54th IEEE Conference on Decision and Control (CDC), Dec 2015, pp. 3161–3168.
- [10] J. T. Hughes, A. D. Domnguez-Garca, and K. Poolla, "Virtual battery models for load flexibility from commercial buildings," in 2015 48th Hawaii International Conference on System Sciences, Jan 2015, pp. 2627–2635.
- [11] I. Chakraborty, S. P. Nandanoori, S. Kundu, and K. Kalsi, *Data-Driven Predictive Flexibility Modeling of Distributed Energy Resources*. Cham: Springer International Publishing, 2020, pp. 311–343.
- [12] K. Amasyali, M. Olama, and A. Perumalla, "A machine learning-based approach to predict the aggregate flexibility of hvac systems," in 2020 IEEE Power Energy Society Innovative Smart Grid Technologies Conference (ISGT), 2020, pp. 1–5.
- [13] S. Kundu, K. Kalsi, and S. Backhaus, "Approximating flexibility in distributed energy resources: A geometric approach," in 2018 Power Systems Computation Conference (PSCC), June 2018, pp. 1–7.
- [14] F. Lin and V. Adetola, "Flexibility characterization of multi-zone buildings via distributed optimization," in 2018 Annual American Control Conference (ACC), June 2018, pp. 5412–5417.
- [15] F. L. Müller, O. Sundström, J. Szabó, and J. Lygeros, "Aggregation of energetic flexibility using zonotopes," in 2015 54th IEEE Conference on Decision and Control (CDC), 2015, pp. 6564–6569.
- [16] S. Barot and J. A. Taylor, "A concise, approximate representation of a collection of loads described by polytopes," *International Journal of Electrical Power & Energy Systems*, vol. 84, pp. 55 – 63, 2017.
- [17] M. S. Nazir, I. A. Hiskens, A. Bernstein, and E. Dall'Anese, "Inner approximation of minkowski sums: A union-based approach and applications to aggregated energy resources," in 2018 IEEE Conference on Decision and Control (CDC). IEEE, 2018, pp. 5708–5715.
- [18] P. Barooah, A. Bušić, and S. Meyn, "Spectral decomposition of demand side flexibility for reliable ancillary service in a smart grid," in 48th Hawaii International Conference on Systems Science (HICSS), January 2015, invited paper.
- [19] D. Wang, K. Ma, P. Wang, J. Lian, and D. J. Hammerstrom, "Frequency-domain flexibility characterization of heterogeneous enduse loads for grid services," in 2020 IEEE Power Energy Society Innovative Smart Grid Technologies Conference (ISGT), 2020, pp. 1–5.
- [20] A. R. Coffman, Z. Guo, and P. Barooah, "Capacity of flexible loads for grid support: statistical characterization for long term planning," in 2020 American Control Conference (ACC), July 2020, pp. 533–538.
- [21] American Society of Heating, Refrigerating and Air-Conditioning Engineers, "The ASHRAE handbook fundamentals (SI Edition)," 2017.
- [22] A. R. Coffman, Z. Guo, and P. Barooah, "Characterizing capacity of flexible loads for providing grid support," arXiv preprint arXiv:2005.01591, 2020.
- [23] A. Rabl, "Parameter estimation in buildings: Methods for dynamic analysis of measured energy use," ASME. J. Sol. Energy Eng., vol. 110, no. 1, pp. 52 – 66, 1988.
- [24] M. Grant and S. Boyd, "CVX: Matlab software for disciplined convex programming, version 1.21," http://cvxr.com/cvx, Feb. 2011.